Physica B 164 (1990) 205–212
North-Holland

RECENT BIOPHYSICAL STUDIES IN HIGH MAGNETIC FIELDS

Georg MARET
Hochfeld Magnetlabor, Max Planck Institut für Festkörperforschung, 166X, F-38042 Grenoble Cedex, France

A brief overview of biophysical effects of steady magnetic fields is given. The need of high field strength is illustrated by several recent diamagnetic orientation experiments. They include rod-like viruses, purple membranes and chromosomes. Results of various studies on bees, quails, rats and pigeons exposed to fields above about 7 T are also resumed.

1. Introduction

Understanding the response of biological matter to magnetic fields has been of scientific interest for a long time. Nowadays the question of a reliable assessment of potential hazards for humans becoming more frequently exposed to fields of increasing strength, for example in NMR tomography, has become an important issue.

The large body of literature has been surveyed with emphasis on different aspects in a number of recent reviews and conference proceedings [1–8]. Various animals such as pigeons, robins, fish and bees respond to magnetic fields below 1 G. Behavioral studies show that some of them use the earth's magnetic field for navigation and homing, but the physical and physiological mechanisms involved in the magnetoreception remain controversial. The discovery of submicron size magnetite particles in tissues of many animals has stimulated the search for a compass needle type detection organ. Clear evidence, however, for the biologically relevant use of such (ferrimagnetic) particles has so far only been provided in the case of magnetotactic bacteria.

Paramagnetic groups are not common in biological matter. Paramagnetic radical pairs are created in some photochemical reactions and the occurrence of triplet states in an external magnetic field may strongly modify the reaction path. In metallo-protein complexes such as the porphyrin group in hemoglobin, myoglobin and chlorophyll, the central iron turns from paramagnetic to diamagnetic on binding of molecular oxygen. This provides not only a convenient means of separating oxygenated from deoxygenated erythrocytes by inhomogeneous magnetic fields, but also to strongly orient deoxygenated crystals of these proteins, as the anisotropic g-factor of the porphyrin group causes a strongly anisotropic paramagnetic susceptibility.

The diamagnetic susceptibility of most organic chemical bonds is also (though much less) anisotropic. This results in magnetic field induced alignment of molecules, macromolecules, larger biological aggregates and liquids with long range orientational correlations such as liquid crystals. In the latter systems full alignment is typically achieved in fields of order 1 T or below, but the detection of orientation effects in the former less correlated liquids may require field strengths well beyond 10 T combined with techniques such as optical birefringence capable of measuring very small alignment. High magnetic fields have thus become a useful tool in the field of complex fluids.

In the first part of this article we illustrate the combined need of high magnetic field strength and high resolution optical techniques by a brief outline of some recent studies on aqueous suspensions of the rod-like virus particles fd and Tobacco Mosaic Virus (TMV), purple membranes and chromosomes. In the second part we resume some recent high field studies on living systems.

2. Rod-like virus particles

The birefringence Δn induced by a magnetic field H perpendicular to the direction of light

propagation in a suspension of rotationally symmetric molecules is given by

$$\Delta n = \left\langle \tfrac{3}{2}\cos^2\theta - \tfrac{1}{2} \right\rangle_f \Delta n_{\mathrm{sat}} . \qquad (1)$$

Δn_{sat} is the difference in refractive index for light polarization parallel and perpendicular to H at complete alignment ($H \to \infty$), θ the angle between the particle's symmetry axis and H, and $\langle\ \rangle_f$ denotes the average over the field dependent orientation distribution function $f(\theta)$. For non-interacting particles with diamagnetic anisotropy $(\chi_{\parallel} - \chi_{\perp}) = \Delta\chi$ in thermal equilibrium

$$f(\theta) = \exp\left[-\left(\frac{\Delta\chi H^2}{2kT} \cos^2\theta \right) \right] . \qquad (2)$$

Hence, for $\Delta\chi H^2 \ll kT$, Δn is proportional to H^2 and amounts to

$$\Delta n = \Delta n_{\mathrm{sat}} \frac{\Delta\chi H^2}{15kT} , \qquad (3)$$

irrespective of the sign of $\Delta\chi$. The coefficient $CM \equiv \Delta n/\lambda H^2$ for $H \to 0$ is defined as the Cotton–Mouton constant. λ is the optical wavelength. For $\Delta\chi H^2 \gg kT$ the quantity $\langle\ \rangle_f$ tends towards 1 or $-\frac{1}{2}$ depending on whether the particles orient with their symmetry axis parallel ($\Delta\chi > 0$) or perpendicular ($\Delta\chi < 0$) to H [9]. For interacting particles the Cotton–Mouton constant becomes proportional to the local orientational order parameter $\langle \frac{3}{2}\cos^2\theta_{ij} - \frac{1}{2} \rangle$, where θ_{ij} denotes the angle between the symmetry axes of the particles i and j. Onsager [10] has pointed out that in suspensions of hard rods an isotropic to "lyotropic" nematic transition should occur as a function of concentration c at a concentration c^* related to the aspect ratio (d/L) of the rods. In Onsager's model the interparticle correlations result in a progressive increase of CM which can be described by a virial expansion [11, 12]. In first order approximation [11], CM reaches an enhancement of about 5 at c^*. The rod-like virus particles fd (length $L = 880$ nm, diameter $d = 6$ nm) and TMV ($L = 300$ nm, $d = 18$ nm) both have substantial diamagnetic and optical anisotropy due to a highly regular anisotropic internal structure, so that CM could be accurately measured in both systems from very low concentrations where correlations are essentially negligible [13–17] up to the isotropic nematic transition [13, 15, 17]. Unfortunately none of the available data sets can be rigorously compared to the theory [11, 12]: fd has an aspect ratio large enough for Onsager's theory to apply, but carries surface charges and appears to have some flexibility [18, 19]. TMV in contrast is almost ideally stiff, but has too low an aspect ratio; it also carries charges and appears difficult to prepare as a monodisperse sample. Recent measurements [17, 20] of both CM and c^* on monodisperse TMV suspensions compare well over the entire range of concentrations and ionic strengths studied, with a recent functional scaling theory [21] for spherocylinders with finite aspect ratio, when the effect of charge is taken into account by an effective diameter. In the above Onsager type models, both interparticle correlations and c^* are temperature independent. The observation [16], that for TMV suspensions well below c^*, CM appears proportional to $(T - T^*)^{-1}$, which is qualitatively similar to thermotropic liquid crystals above the isotropic nematic transition, rather than proportional to T^{-1} as expected from eq. (3) for an athermal system, seems therefore striking. We have also found this stronger temperature dependence [20], but, in addition, that T^* is independent of c. This argues against temperature dependent *inter*particle effects and may indicate a T dependence of $\Delta\chi$ and/or Δn_{sat} perhaps due to *intra*particle structural rearrangements.

At concentrations above c^* the long range correlations in the lyotropic nematic phase allow strong macroscopic alignment in fields of order 1 T [2, 7, 14, 22, 23]. The orientational distribution function becomes strongly peaked about the field axis [24], the remaining small disalignment being due to (small) thermal orientational fluctuations.

As below c^* the magnetic alignment is weak the *dynamic* properties are hardly affected by the presence of the magnetic field. At concentrations well above 1 rod/L^3 but below c^* the self-diffusion coefficient of the rods becomes smaller than

the Stokes value for free rods mainly because diffusion perpendicular to the rod axes is hindered by the presence of essentially randomly oriented neighboring rods. The local anisotropy of the self-diffusion cannot be measured because the macroscopic diffusion remains isotropic. Due to the ease of magnetic alignment above c^*, however, the anisotropy can be conveniently measured in this case using optical labelling techniques. Figure 1 shows schematically the experimental set-up of a modified version of the fringe pattern fluorescence bleaching technique [25] combined with a horizontal room temperature superconducting magnet used [26] to study anisotropic diffusion in lyotropic suspensions of fd and TMV. A fraction of the particles studied are covalently labelled with fluorescein-isothiocyanate, a dye whose green fluorescence can be partly bleached by a pulse of intense ($\simeq$ W/mm^2) laser light at $\lambda = 488$ nm. The same beam at a low power, which is controlled by a Pockels cell between two crossed polarizers, is used to monitor the remaining fluorescence after bleaching. The distance $a = 2\pi/q$ over which diffusion is probed is given by the interference fringe spacing produced at the sample by crossing two beams split after the second polarizer. The relaxation of the spatially periodic concentration profile of fluorescent particles after the bleach pulse is measured by slight modulation of the position of the reading fringe pattern using a piezoelectrically driven mirror and lock-in detection of the modulated part of the fluorescence signal. With the help of additional mirrors the direction of q can be oriented parallel or perpen-

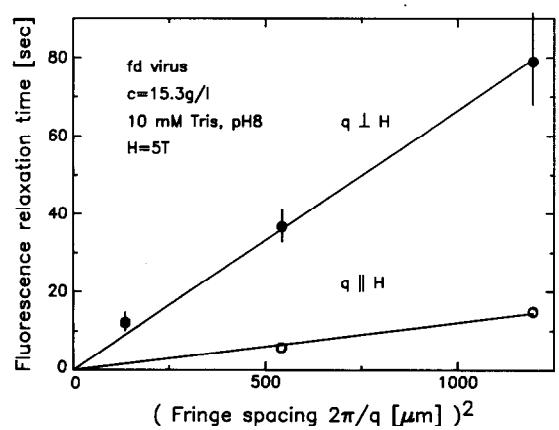

Fig. 2. The relaxation time of the modulated fluorescence signal versus the square of the fringe spacing a. Aqueous lyotropic suspension of magnetically oriented rod-like virus fd, $T = 27$°C, $c = 15.3$ mg/ml, 10 mM Tris–HCl buffer at pH 8, $H = 5$ T [26].

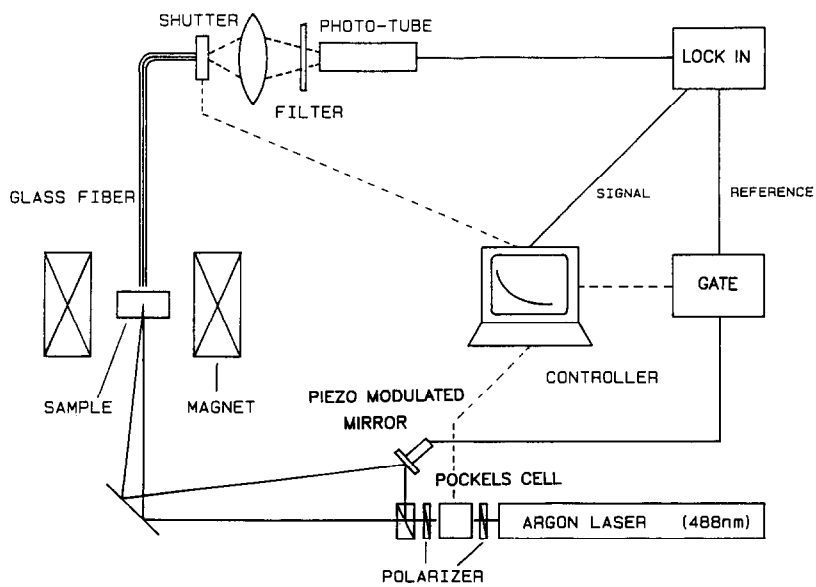

Fig. 1. Fringe pattern fluorescence bleaching experiment to measure anisotropic self-diffusion in magnetically oriented samples.

dicular to H and the component of the self-diffusion constant parallel and perpendicular to the average rod direction measured. In fig. 2 we show the relaxation time of the modulated fluorescence signal as a function of a^2 for both geometries, from a magnetically oriented lyotropic suspension of fd at a concentration of 15.3 mg/ml. The self-diffusion is much faster along the magnetic field than perpendicular, revealing the essentially free motion of the particles along their rod axis. The perpendicular motion is mostly hindered because of the orientational fluctuations of the neighboring rods.

3. Light induced structural changes in purple membranes

Lipid membranes generally orient with the membrane plane parallel to the magnetic field (see e.g. ref. [2]) because of the overall negative $\Delta\chi$ of the constituent hydrocarbon chains and their high internal liquid crystal type order. In membrane protein complexes such as retinal rods [27] or purple membranes of *Halobacterium halobium* [28], however, the dominant contribution to the diamagnetic anisotropy stems from the α-helical protein segments essentially aligned normal to the membrane plane, and from aromatic amino acids. These membranes therefore orient with the normal parallel to H [28, 29]. Because of the regular alignment of the α-helical parts and/or aromatic groups of the protein bacteriorhodopsin (BR) in the purple membrane, half micron sized membrane sheets reach sufficient alignment in magnetic fields of 12 T to show an onset of saturation of the field induced birefringence [28]. This is illustrated in fig. 3 [30]. The curvature visible in this plot does not exactly follow the prediction of eqs. (1) and (2) because of the spread in membrane size typical for such samples [28]. Nevertheless it appears clear from this figure that almost complete alignment is reached in fields between 20 and 25 T. Thus it is possible to determine Δn_{sat} from the high field saturation behavior and then to obtain $\Delta\chi$ from the low field slope $CM \propto \Delta\chi\,\Delta n_{sat}$. For structurally anisotropic particles, changes in $\Delta\chi$ may

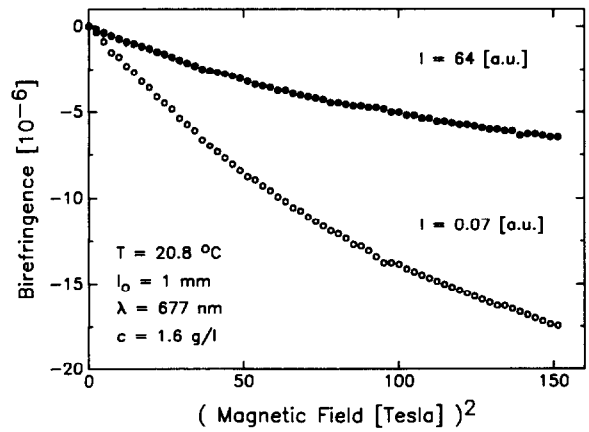

Fig. 3. Magnetic birefringence measurement of an aqueous suspension of purple membrane sheets, $c = 1.6$ mg/ml in 6 M guadinium chloride at two different intensities I of the laser beam, corresponding to the BR_{568} state (at $I = 0.07$) and the M_{415} state ($I = 64$) in the photocycle of bacteriorhodopsin [30].

sensitively reflect internal conformational changes as illustrated by earlier work on the bacteriophage Pf1 [14].

Bacteriorhodopsin acts as a proton pump across the purple membrane driven by light absorption. Whether this light induced transport is associated with sizeable conformational changes in the bacteriorhodopsin molecule remained highly controversial, exept for the well known all-*trans* to 13-*cis* isomerisation of the chromophore retinal. Dresselhaus et al. [30] have addressed this question with magnetic birefringence. In the presence of guadinium the lifetime of the so-called intermediate M_{415}-state of the photocycle of BR is sufficiently enhanced so that the system can be monitored continuously in the ground state BR_{568}, or in the M_{415} state, respectively, at low and high intensity of the measuring Kr^+ laser at $\lambda = 677$ nm. Figure 3 shows the dramatic, about 2.7-fold change of the magnetic birefringence on tuning up the laser power. In fig. 4 we plot the Cotton–Mouton constant as a function of the laser intensity. The intensity independent states observed at low and high intensities correspond to the BR_{568} and M_{415} states, respectively. The change in CM cannot be directly attributed to a change in $\Delta\chi$, since Δn_{sat} also differs in both states because of

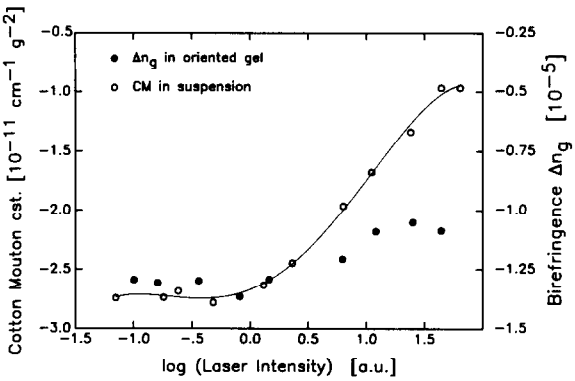

Fig. 4. The Cotton–Mouton constant *CM* of the purple membrane sample described in fig. 3 and the birefringence Δn_g of a gel with fixed orientation of the sheets as a function of the laser intensity [30].

the large shift of the optical absorption band from a peak position of 568 nm in BR_{568} to 415 nm in M_{415}. The relative change in Δn_{sat} was measured in zero field on the same sample after locking the magnetic alignment of the membrane sheets by polymerization of a polyacrylamid gel under a field of 12.3 T. This gentle technique provides well oriented stable specimens, as demonstrated by the neutron small angle diffraction pattern from such a sample (fig. 5) and appears very useful in many other applications

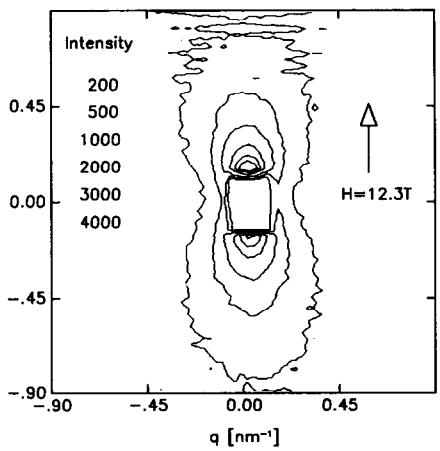

Fig. 5. Contour plot of the neutron small angle scattering intensity (taken at the diffractometer D11 at the Institut Laue–Langevin, Grenoble) of a magnetically oriented suspension of the purple membrane. The orientation was produced by a vertical magnetic field and locked by gelation under field using 30% by weight polyacrylamide [30].

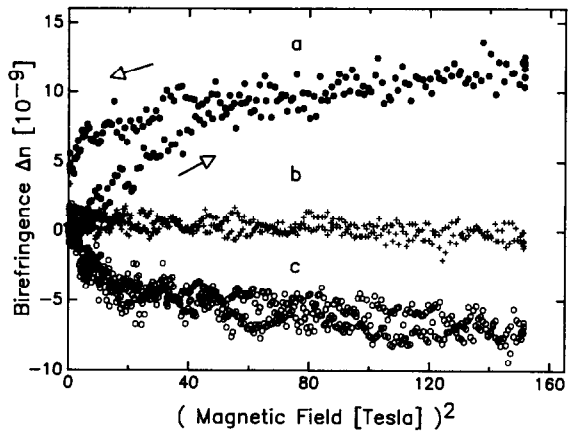

Fig. 6. Magnetic birefringence from suspensions of metaphase chromosomes [34]. (a) Chinese hamster lung chromosomes, $c \simeq 12$ μg/ml DNA, polyamine buffer [34, 35], (b) destroyed CHL chromosomes, hexandiol buffer [34, 35], 4.5% SDS. (c) Human lymphocyte chromosomes, $c \simeq 8$ μg/ml DNA, 30% sucrose [34].

[2]. The light induced change of the birefringence Δn_g of the gel, which is proportional to Δn_{sat}, amounts to about 20% (fig. 4). These measurements therefore clearly reveal a more than 2 times higher $\Delta\chi$ of the purple membrane sheet in the BR_{568} state than in the M_{415} state, suggesting a substantial light induced conformational change of bacteriorhodopsin.

4. Chromosomes

Metaphase chromosomes are a condensed phase of the desoxyribonucleic acid (DNA) protein complex called chromatin [31]. It is currently believed that the packing of chromatin inside the metaphase chromosomes is highly regular, but the chromosome structure is not known in detail. The DNA double helix is spooled around the globular histones in about two turns forming the so-called 11 nm diameter nucleosomes. Including the DNA segment linking two nucleosomes, this takes about 200 basepairs of DNA ($\simeq$ 68 nm length) per nucleosome. Chromatin fibers of 30 nm diameter are built up by helically interwound chains of the nucleosomes. These fibers form, on average over the different chromosomes, about 2600 extended loops con-

taining about 460 nucleosomes each and pointing mostly radially from the long axis of the chromosome [31].

From the Cotton–Mouton effect of DNA [32], of chromatin and of nucleosomes [33], which has been investigated earlier, one can estimate the magnetic orientation behavior of metaphase chromosomes based on the above model for the internal structure. For this we use the nucleosome particle as the fundamental anisotropic subunit. Its diamagnetic anisotropy $\Delta\chi_n$ can be roughly approximated by the value for 200 basepairs (with anisotropy $\Delta\chi_{BP} = -1.7 \times 10^{-28}$ cgs [32]) wound as a helix with a pitch angle of about 15°, $\Delta\chi_n \simeq -0.39$, $200\,\Delta\chi_{BP} \simeq 1.3 \times 10^{-26}$ cgs per nucleosome, since the contribution of the almost spherical protein core is negligible [33]. Assuming no form birefringence of the nucleosome, the same helical arrangement of DNA gives $\Delta n_{sat,n} \simeq 0.039\,cm^3/g$, and hence $CM_n \simeq 1.3 \times 10^{-11}$ cgs in fair agreement with the experimental value 1×10^{-11} cgs [33].

In order to estimate $\Delta\chi_c$ and $\Delta n_{sat,c}$ of a metaphase chromosome, we assume that 370 of the 460 nucleosomes in a loop of the chromatin fiber point with their helical symmetry axis radially with respect to the chromosome long axis, as suggested by structural models in the literature [31]. This accounts for 90 nucleosomes in the turning parts of a loop, the anisotropies of which cancel. This estimate gives $\Delta\chi_c \simeq -6.2 \times 10^{-21}$ cgs per particle, $\Delta n_{sat,c} \simeq -0.016\,cm^3/g$ and $CM_c \simeq 2.6 \times 10^{-6}$ cgs (at a concentration of $1\,g/cm^3$). At such large $\Delta\chi$ values the magnetic birefringence is expected from eqs. (1) and (2) to deviate appreciably from the H^2 law at fields $H \geq 0.36$ T, the field at which $\Delta\chi H^2/2kT$ equals 1. Following this estimate, essentially full orientation (Δn at 90% of saturation $\equiv -0.45\,\Delta n_{sat}$) of chromosomes should thus be achieved in fields of about 1.4 T. In addition the birefringence of a chromosome suspension containing 8 μg/ml DNA should saturate in high fields towards $\Delta n_{sat,c} \simeq 7 \times 10^{-8}$, a value easily detectable.

Optical birefringence experiments on chromosome suspensions are restricted to very small concentrations for the strong light scattering of these several micrometer sized particles. Figure 6 shows first measurements [34] on Chinese hamster lung (CHL) chromosomes and human lymphocyte chromosomes at $\simeq 12$ μg/ml and $\simeq 8$ μg/ml equivalent DNA concentration, respectively. The high noise level in the data originates from parasitic depolarized light scattering. Also shown for comparison is the measurement from a similar preparation of CHL chromosomes, where the chromosomes were destroyed by addition of the ionic detergent SDS. In curve (a) the field sweep rate of $\simeq 0.1$ T/s was too high to allow complete rotation of the chromosomes into the thermal equilibrium orientation distribution corresponding to each field value. Both samples (a) and (c) exhibit some saturation, but at field strengths more than one order of magnitude higher than the values estimated above. In addition the observed Δn_{sat} values ($\simeq 10^{-8}$) are one order of magnitude smaller than estimated. Consistently, the observed value $CM_c \simeq 7 \times 10^{-9}$ cgs is about 400 times smaller than the estimate. This indicates that the internal packing of DNA in the chromosomes is much less anisotropic then suggested by the above model. It appears in fact that most of the diamagnetic and optical anisotropy cancels and the remaining small part may have different values depending in a reproducible and systematic way on sample preparation, solvent conditions and type of chromosome [34]. A more quantitative analysis of the present results appears difficult for the inherent polydispersity and polymorphism of the non-fractionated natural chromosome suspensions used.

5. Living systems

Among the more striking recent reports of effects of strong steady magnetic fields on living systems are temperature changes up to several degrees found in man [36], mice [37], and pigeons [38], and a strongly oriented growth of monocellular pollen tubes [39]. Whereas the latter phenomenon still deserves a microscopic explanation, the former has been shown for the pigeons [40] to originate from magnetic field induced changes of the thermal convection pattern in the surrounding air due to the force on

paramagnetic molecular oxygen in the magnetic field gradient. Consistently, experiments on man [41] and mice [42] in substantially more homogeneous fields have failed to detect temperature changes. Sensory evoked potentials in the brain also appear affected by fields in the tesla range [43].

Recently, extended series of experiments have been performed on quails [44], bees [45], and rats [46] to settle whether embryonic development may proceed normally in fields above 5 T. Quail eggs exposed after fertilization for 3 or 16 days continuously to fields between 0.8 and 6.4 T hatched normally and behavioral and morphological investigations of the animals did not show any significant difference to unexposed controls [44]. A similar study was performed on eggs and pupae of bees [45]. As an example the typical result of one out of numerous similar egg hatching experiments is shown in fig. 7. The experimental group of bee eggs was kept during the entire breeding period in a superconducting solenoid at 6.78 T, and a first control group in an identical housing at the same temperature, humidity, pressure, etc., outside the magnet. A second control group was placed in a conventional incubator in another laboratory. No significant differences were observed in the total number of hatched eggs, nor in the average time of gestation (fig. 7), nor in the average weight of the pupae. Similar results were obtained in the series of bee emergence experiments.

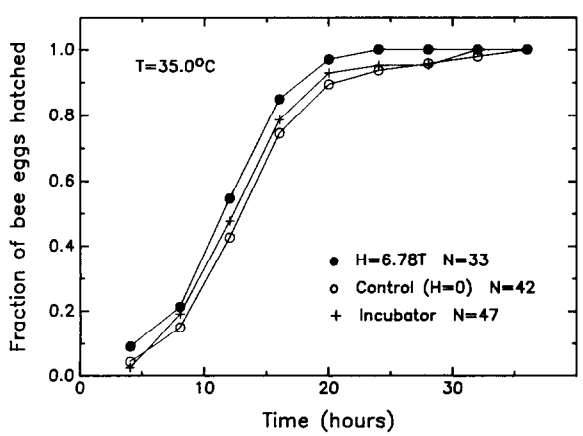

Fig. 7. Time dependence of cumulative number of bee eggs hatched at the end of the gestation period [45].

In another experiment [46], 11 pregnant rats were kept as a group within a four storey 40 cm diameter and 60 cm height cylindrical container with free access to food and tap water inside the large bore superconducting part of the Grenoble hybrid magnet. The rats were exposed during gestational days 12–16, a period of major organogenesis, to 10 T central field for 8 h/day. Controls were kept in identical housings under identical conditions both near the magnet and in another laboratory. Various quantities such as pregnancies, litter size and weight, sex ratio, organ weights and learning abilities of the dams after delivery revealed no significant difference between the experimental group and the controls.

These experiments, as well as an earlier study of frog embryos in 1 T [47], suggest that steady magnetic fields of strengths well above values currently used in NMR tomography may not severely interfere with normal embryonic development, at least in the different types of animals investigated.

References

[1] T.S. Tenforde, ed., Magnetic Field Effects on Biological Systems (Plenum, New York, 1979).
[2] G. Maret and K. Dransfeld, in: Topics in Applied Physics, Vol. 57, F. Herlach, ed. (Springer, Berlin, 1985).
[3] C. Polk and E. Postow, eds., CRC Handbook of Biological Effects of Electromagnetic Fields (CRC Press, Boca Raton, FL, 1986).
[4] J.L. Kirschvink, D.S. Stones and B.J. MacFadden, eds., Magnetite Biomineralization and Magnetoreception in Organisms: A New Biomagnetism (Plenum, New York, 1986).
[5] J.H. Bernardt, ed., Biological Effects of Static and Extremely Low Frequency Magnetic Fields, BGA Schriften 3/86 (MMV Medizin Verlag, München, 1986).
[6] G. Maret, J. Kiepenheuer and N. Boccara, eds., Biophysical Effects of Steady Magnetic Fields, Springer Proc. Phys. Vol. 11 (Springer, Berlin, 1986).
[7] J. Torbet, Trends Biochem. Sci. 12 (1987) 327.
[8] R.M. Burgoyne, ed., Proc. Cardiff Conf. Orientation and Navigation. Birds, Humans and other Animals (The Royal Institute of Navigation, London, 1989).
[9] J.L. Shaw, J. Phys. Chem. 67 (1963) 2215.
[10] L. Onsager, Ann. N.Y. Acad. Sci. 51 (1949) 627.
[11] J.P. Straley, Mol. Cryst. Liq. Cryst. 22 (1973) 333.

[12] P. Photinos and A. Saupe, Mol. Cryst. Liq. Cryst. 123 (1985) 217.
[13] G. Maret, J. Torbet, E. Senechal, A. Domard, M. Rinaudo and M. Milas, in: Nonlinear Behaviour of Molecules, Atoms and Ions in Electric, Magnetic or Electromagnetic Fields, L. Neel, ed. (Elsevier, Amsterdam, 1979) p. 477.
[14] J. Torbet and G. Maret, Biopolymers 20 (1981) 2657.
[15] H. Nakamura and K. Okano, Phys. Rev. Lett. 50 (1983) 186.
[16] D. Photinos, C. Rosenblatt, T.M. Schuster and A. Saupe, J. Chem. Phys. 87 (1987) 6740.
[17] S. Fraden, G. Maret, D.L.D. Caspar and R.B. Meyer, Phys. Rev. Lett. 63 (1989) 2068.
[18] E. Loh, Biopolymers 8 (1979) 2549.
[19] T. Maeda and S. Fujime, Macromolecules 18 (1985) 2430.
[20] S. Fraden, G. Maret, D.L.D. Caspar and R.B. Meyer, to be published.
[21] S.D. Lee, J. Chem. Phys. 87 (1987) 4972.
[22] R. Oldenbourg, Thesis Universität Konstanz, 1981.
[23] S. Fraden, A.J. Hurd, R.B. Meyer, M. Cahoon and D.L.D. Caspar, J. de Phys. 46 (1985) C3–85.
[24] R. Oldenbourg, X. Wen, R.B. Meyer and D.L.D. Caspar, Phys. Rev. Lett. 61 (1988) 1851.
[25] J. Davoust, P.F. Devaux and L. Leger, EMBO J. 1 (1982) 1233.
[26] J. Peetermans, G. Federle and G. Maret, to be published.
[27] M. Chabre, Proc. Natl. Acad. Sci. USA 75 (1978) 5471.
[28] B. Lewis, L.C. Rosenblatt, R.G. Griffin and J. Courtemanche, Biophys. J. 47 (1985) 143.
[29] D.C. Neugebauer, A.E. Blaurock and D.L.D. Worcester, FEBS Lett. 78 (1977) 31.
[30] D. Dresselhaus, Thesis Techn. Universität Berlin, 1988.
N.A. Dencher, D. Dresselhaus, G. Maret, G. Papadopoulos, G. Zaccai and G. Büldt, Proc. Yamada Conf. XXI (1988) p. 109.
D. Dresselhaus, N.A. Dencher and G. Maret, to be published.
[31] K.E. van Holde, Chromatin, Springer, Berlin, 1988.
B. Alberts, D. Bray, J. Lewis, M. Raff, K. Roberts and J. Watson, Molecular Biology of the Cell (Garland, New York, 1983).
[32] G. Maret and G. Weill, Biopolymers 22 (1983) 2727.
[33] G. Maret and K. Dransfeld, Physica B 86–88 (1977) 1077.
[34] F. Hauert, Diplomarbeit, Universität Heidelberg, 1988.
F. Hauert, F. Bier, C. Cremer and G. Maret, unpublished.
[35] A.K Sharma and A. Sharma, Chromosome Techniques (Butterworth, London, 1980).
[36] H. Gremmel, H. Wendhausen and F. Wunsch, Z. Phys. Baln. Med. Klin. 14 (1985) 160.
H. Wendhausen et al., Zbl. Radiol. 128 (1984) 119.
F. Wunsch, in ref. [6], p. 125.
[37] D. Sperber, R. Oldenbourg and K. Dransfeld, Naturwissenschaften 71 (1984) 100.
[38] J. Ecochard, G. Maret and J. Kiepenheuer, Naturwissenschaften 73 (1986) 43.
[39] D. Sperber, K. Dransfeld, G. Maret and M.H. Weissenseel, Naturwissenschaften 68 (1981) 40.
[40] J. Ecochard and G. Maret, in ref. [6], p. 132.
G. Maret and J. Ecochard, Phys. Scripta T13 (1986) 169.
J. Ecochard and G. Maret, Naturwissenschaften 74 (1987) 39.
[41] F.G. Shellock, D.J. Schaeffer and G.J. Gordon, Magn. Res. Med. 3 (1986) 644.
[42] T.S. Tenforde, Bioelectromagnetics 7 (1986) 3.
[43] L. von Klitzing, E. Ihnen and B. Terwey, Naturwissenschaften 71 (1984) 538.
L. von Klitzing, in ref. [6], p. 122.
L. von Klitzing, H. Gerhard, U. Benthin and J. Jörg, Z. EEG EMG 18 (1987) 43.
L. Stojan, D. Sperber, W. Sommer and K. Dransfeld, Naturwissenschaften 75 (1988) 622.
[44] J. Bouvet and G. Maret, in ref. [6], p. 138.
[45] J. Kefuss and J. Ecochard, to be published.
[46] M. Bornhausen, J. Ecochard and G. Maret, to be published.
[47] S. Ueno, K. Harada and K. Shiokawa, IEEE Trans. Magn. MAG-20 (1984) 1663.